V. Conclusions

In this first set of experiments at a frequency near 400 MHz with a liquid cooler applicator, we were able to verify the following.

a) At a depth of 4 cm or more, an efficient hyperthermic level was reached.

b) The maximum temperature can be shifted ad hoc from the surface to a depth of approximately 3 cm.

c) A quasi-constant hyperthermic level about 4 cm thick (starting from surface) can be obtained by controlling the cooling water temperature and RF power. Alternatively, one can perhaps keep constant (colder) water temperature and simultaneously operate on less deep strata by a second RF generator working at higher frequency which is less penetrating (the applicator is able to perform this test).

d) a), b), and c) results seem interesting also for clinical cases, but it must be recalled that all tests were made on carefully selected homogenous living tissue (also on two animals of different weights). So, much more caution is necessary, and it is important to get the best possible map of inner temperature distribution.

References

[1] T.C. Cetas, W.G. Conner, and M.L.M. Boone, "Thermal dosimetry: Some biophysical considerations," *Cancer Therapy by Hyperthermia and Radiation*, p. 3, 1978.

[2] D.A. Christensen and C.H. Durney, "Hyperthermia production for cancer therapy: A review of fundamentals and methods," *Microwave Power*, vol. 16, p. 2, 1981.

[3] G.M. Hahn, P. Kernahan, A. Martinez, D. Pounds, and S. Prionas, "Some heat transfer problems associated with heating by ultrasound, microwaves, or radiofrequency" *Ann NY Acad. Sci*, vol. 335, pp. 327–346, 1980.

[4] J. Mendecki, E. Friedenthal, C. Botstein, F Sterzer, R Paglione, M. Nowogrodzki, and E. Beck, "Microwave induced hyperthermia in cancer treatment. Apparatus and preliminary results," *Int. J. Radiat. Oncol. Biol. Phys.*, vol. 4, pp. 1095–1103, 1978.

[5] T.S. Sandhu, H.S. Kowal, and R.J.R. Johnson, "The development of microwave hyperthermia applicators," *Int. J. Radiat. Oncol Biol Phys.*, vol. 4, pp. 515–519, 1978.

Multi-Octave Performance of Single-Ended Microwave Solid-State Amplifiers

KARL B. NICLAS, SENIOR MEMBER, IEEE

(Invited Paper)

***Abstract*—The computed performances of multi-stage single-ended GaAs MESFET amplifiers are compared when employing one and the same transistor type. The circuit principles studied are of the reflective match, the lossy match, the feedback, the distributed, and the active-match amplifier variety. It was found that the gain characteristics of the single-stage modules using either passive or active matching do not conclusively identify the optimum circuit type in the band of interest (2–18 GHz). For the case of multistage devices, however, the gain and the VSWR performance clearly favor the distributed amplifier principle.**

In addition to the data reported in the literature, the paper discusses recent experimental results obtained from a 3–17.5-GHz reflective match module, a two-stage 2–18-GHz and a four-stage 0.5–18.5-GHz feedback amplifier, as well as a two-stage 2–20-GHz and a four-stage 2–18-GHz distributed amplifier.

I. Introduction

THE CONCEPT of the balanced reflective match amplifier has dominated the design of microwave solid-state amplifiers for nearly two decades [1]. Up to this day, quadrature hybrids of the type invented by J. Lange [2] are almost exclusively occupying the position of the signal combiner and divider yielding excellent performance, regardless of the mismatch presented by the two identical single-ended modules. However, the bandwidth of the balanced reflective match amplifier is limited to two octaves, at best. Extending the frequency band beyond this 4:1 ratio requires a minimum of three 90° couplers in tandem configuration [3]–[5]. Unfortunately, these tandem couplers are not only complicated, but space-consuming and costly to manufacture. Due to these reasons and their cost effectiveness, multi-octave single-ended amplifiers are gaining more and more in importance. Four circuit design principles exhibiting excellent ultra-wideband characteristics are now challenging the concept of the balanced reflective match amplifier [6]–[30]. Hence, the five competitors are:

1) the reflective match amplifier,

Manuscript received December 16, 1983; revised March 5, 1984.

The author is with the Watkins–Johnson Company, Stanford Industrial Park, Palo Alto, CA 94304.

0018-9480/84/0800-0896$01.00 ©1984 IEEE

2) the lossy match amplifier,
3) the feedback amplifier,
4) the distributed amplifier, and
5) the active match amplifier.

While the first four circuit types employ passive elements to improve the input and output matches, the fifth principle makes use of active elements to achieve the same goal [9]–[13]. Characterized by their simplicity, compact size, and low cost, single-ended amplifiers represent attractive options whenever an economical solution to wide-band amplification is of primary concern.

Finding the optimum solution from these five circuit types poses, however, a difficult problem and has no simple answer. In an attempt to compare the performance characteristics of these alternatives, one needs to establish certain conditions to arrive at a meaningful solution. To keep matters simple, we chose only the following two:

1) all amplifiers use identical active devices independent of the circuit type employed, and
2) the frequency band of interest is 2–18 GHz.

The limiting conditions are necessary since, among other factors, the electrical performance of each circuit principle depends greatly on the transistor type and the desired bandwidth. Either factor may have a decisive impact on the choice of the optimum design concept. Confining the comparison to a specific device type and a particular frequency band may seem to lack the depth expected from such an analysis. However, the removal of these restrictions would render our study rather unmanageable and, therefore, beyond the scope of this paper.

II. Computed Results

A. Matching with Passive Elements

In the following, we compare the performance characteristics of the reflective match (*RM*), the lossy match (*LM*), the feedback (*FB*), and the distributed amplifier (*DA*) based on computed results. The individual circuits are optimized for gain, gain flatness, and reflection coefficients. All passive elements are realizable, although some high-impedance lines may be difficult to manufacture. As already pointed out, the frequency band extends from 2 to 18 GHz and identical GaAs MESFET's are being used in all circuit types. The transistor's model and its element values are presented in Fig. 1. The latter have been obtained from the measured *S*-parameters of a GaAs MESFET with a 0.5×300-μm gate and a $2 \cdot 10^{17}$ cm^{-3} carrier concentration.

The topologies of the amplifier modules and the values of their components are presented in Fig. 2. Biasing can be accomplished easily through any of the short-circuited shunt elements. However, this causes a loss in efficiency in case a resistor is part of the biasing network. The values of all passive circuit components have been optimized for best gain performance and do not represent the optimum conditions for noise figure. The positions of the active device in both the lossy match and the feedback amplifier are occupied by two GaAs MESFET's in parallel. This is due to

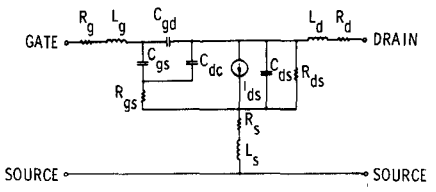

INTRINSIC ELEMENTS		EXTRINSIC ELEMENTS	
gm	= 28 mS	R_g	= 1 ohm
τ_0	= 5.2 psec	L_g	= .085 nH
C_{gs}	= .25 pF	R_s	= .44 ohm
C_{gd}	= .012 pF	L_s	= .041 nH
C_{dc}	= .014 pF	C_{ds}	= .066 pF
R_{gs}	= 5.2 ohm	R_d	= 1 ohm
R_{ds}	= 272 ohm	L_d	= .346 nH

Fig. 1. Half-micron gate FET model and its element values.

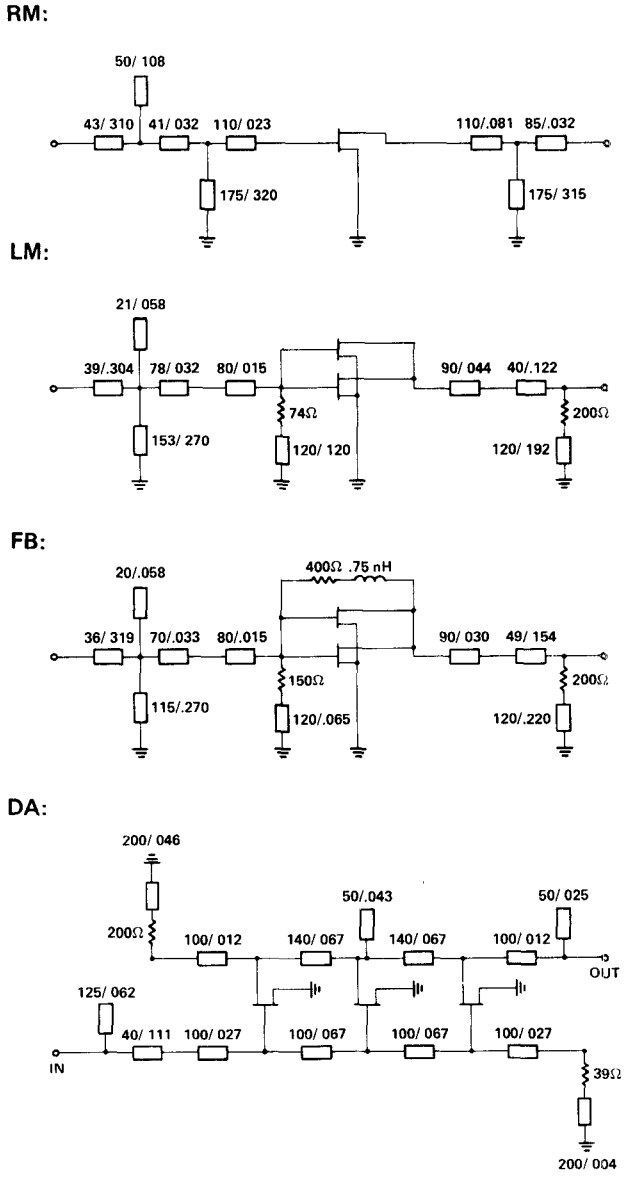

Fig. 2. Circuit topologies of the single-ended amplifier modules (lengths of transmission lines in inches for air dielectric).

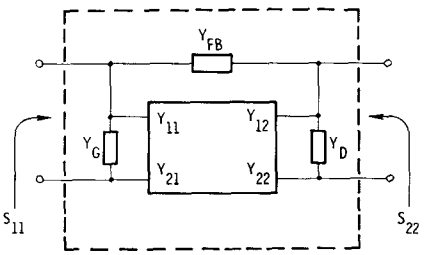

$$S_{21} = -\frac{Y_0}{Y_{12}-Y_{FB}}\left[\sqrt{1+\frac{(Y_{21}-Y_{FB})(Y_{12}-Y_{FB})}{Y_0^2}\left(1+S_{11}\right)\left(1+S_{22}\right)}-1\right]$$

Fig. 3. Two-port with lossy match and feedback components.

the insufficient gain produced by the single device of Fig. 1 for these types of circuits, as will be further explained below.

The insertion gain of a single-ended module making simultaneous use of lossy matching and feedback (Fig. 3) may be expressed by [6]

$$\text{GAIN} = \left|\frac{Y_0}{(nY_{12}-Y_{FB})}\left[\sqrt{1+\frac{(nY_{21}-Y_{FB})(nY_{12}-Y_{FB})}{Y_0^2}(1+S_{11})(1+S_{22})}-1\right]\right|^2 \tag{1}$$

when n parallel transistors are employed. The module's reflection coefficients are

$$S_{11} = \frac{(Y_0-Y_{11}')(Y_0+Y_{22}')+(nY_{21}-Y_{FB})(nY_{12}-Y_{FB})}{(Y_0+Y_{11}')(Y_0+Y_{22}')-(nY_{21}-Y_{FB})(nY_{12}-Y_{FB})} \tag{1a}$$

$$S_{22} = \frac{(Y_0+Y_{11}')(Y_0-Y_{22}')+(nY_{21}-Y_{FB})(nY_{12}-Y_{FB})}{(Y_0+Y_{11}')(Y_0+Y_{22}')-(nY_{21}-Y_{FB})(nY_{12}-Y_{FB})} \tag{1b}$$

$$Y_{11}' = nY_{11}+Y_G+Y_{FB} \tag{1c}$$

$$Y_{22}' = nY_{22}+Y_D+Y_{FB} \tag{1d}$$

$$Y_0 = Z_0^{-1}. \tag{1e}$$

At low frequencies ($B_{FB} \ll G_{FB}$, $Y_{21} \simeq g_m$) and $nY_{12} \ll G_{FB}$, the set of equations (1) reduces to

$$\text{GAIN} \cong \left[\frac{Y_0}{G_{FB}}\left[\sqrt{1-(ng_m-G_{FB})G_{FB}Z_0^2(1+S_{11})(1+S_{22})}-1\right]\right]^2 \tag{2}$$

$$S_{11} \cong \frac{(Y_0-Y_{11}')(Y_0+Y_{22}')-(ng_m-G_{FB})G_{FB}}{(Y_0+Y_{11}')(Y_0+Y_{22}')+(ng_m-G_{FB})G_{FB}} \tag{2a}$$

$$S_{22} \cong \frac{(Y_0+Y_{11}')(Y_0-Y_{22}')-(ng_m-G_{FB})G_{FB}}{(Y_0+Y_{11}')(Y_0+Y_{22}')+(ng_m-G_{FB})G_{FB}} \tag{2b}$$

$$Y_{11}' \cong G_G+G_{FB} \tag{2c}$$

$$Y_{22}' \cong nG_{ds}+G_D+G_{FB} \tag{2d}$$

(G_{ds}—drain-to-source conductance.)

For $n=2$, $g_m=28$ mS, $G_{ds}=3.7$ mS, $G_{FB}=2.5$ mS, $G_G=6.7$ mS, and $G_D=5$ mS [Fig. 2 (FB)] we calculate with (2) a gain of $G=5.3$ dB and the reflection coefficients $|S_{11}|=0.21$ and $|S_{22}|=0.02$. The corresponding parameters for $n=1$ are $G=0.3$ dB, $|S_{11}|=0.28$, and $|S_{22}|=0.20$, representing an unacceptably low gain response. Similar results exist for the LM circuit of Fig. 2, for which (1) assumes the following low-frequency expressions [6]

$$\text{GAIN} \cong \frac{1}{4}\left[ng_mZ_0(1+S_{11})(1+S_{22})\right]^2 \tag{3}$$

$$S_{11} \cong \frac{Y_0-G_G}{Y_0+G_G} \tag{3a}$$

$$S_{22} \cong \frac{Y_0-(nG_{ds}+G_D)}{Y_0+(nG_{ds}+G_D)}. \tag{3b}$$

For $n=2$, $g_m=28$ mS, $G_G=13.5$ mS, and $G_D=5$ mS, we calculate with (3) $G=6.2$ dB, $|S_{11}|=0.19$, and $|S_{22}|=0.24$. In the case of $n=1$, the gain is reduced to $G=1.2$ dB with $|S_{11}|=0.19$ and $|S_{22}|=0.40$. As discussed elsewhere, (3) also represents the gain and the reflection coefficients of a distributed amplifier at low frequencies when n links are employed [7]. In order to achieve an equivalent gain with the distributed amplifier, three links are required.

In the following, we will show that similar gain performance may be obtained with the four circuits illustrated in Fig. 2. Their small signal gains, noise figures, and reflection coefficients are plotted in Fig. 4 across the band of interest. While the average gains of all four amplifier types remain within 1.6 dB of each other, the reflection coefficients exhibit vast differences. The latter, more than any other parameters, dictate the feasibility of the design principle in the case of multistage operation. The average noise figures of the four types stay within 1.1 dB of each other. Table I summarizes the performance characteristics of the 2–18-GHz modules. Comparing the data, the distributed amplifier demonstrates the best gain flatness, the lowest reflection coefficients, and the highest stability factors. Its maximum noise figure, however, exceeds those of the other modules. The lossy match amplifier shows the best overall noise figure in addition to excellent gain performance. The feedback amplifier trails both the lossy match and the distributed amplifier in gain, but has the advantage of lower reflection coefficients over the LM unit. In contrast, the RM module is unstable at frequencies below 9 GHz and, therefore, not very well suited for cascading.

As already pointed out, the choice of the circuit type is mostly dictated by the reflection coefficients, for they represent the most critical parameters. The importance of the modules' input and output VSWR becomes very much apparent when cascading several units. The impact on gain, gain flatness, maximum VSWR, and stability factor is summarized in Table II. While the gain characteristics of both the feedback and the distributed amplifier may be

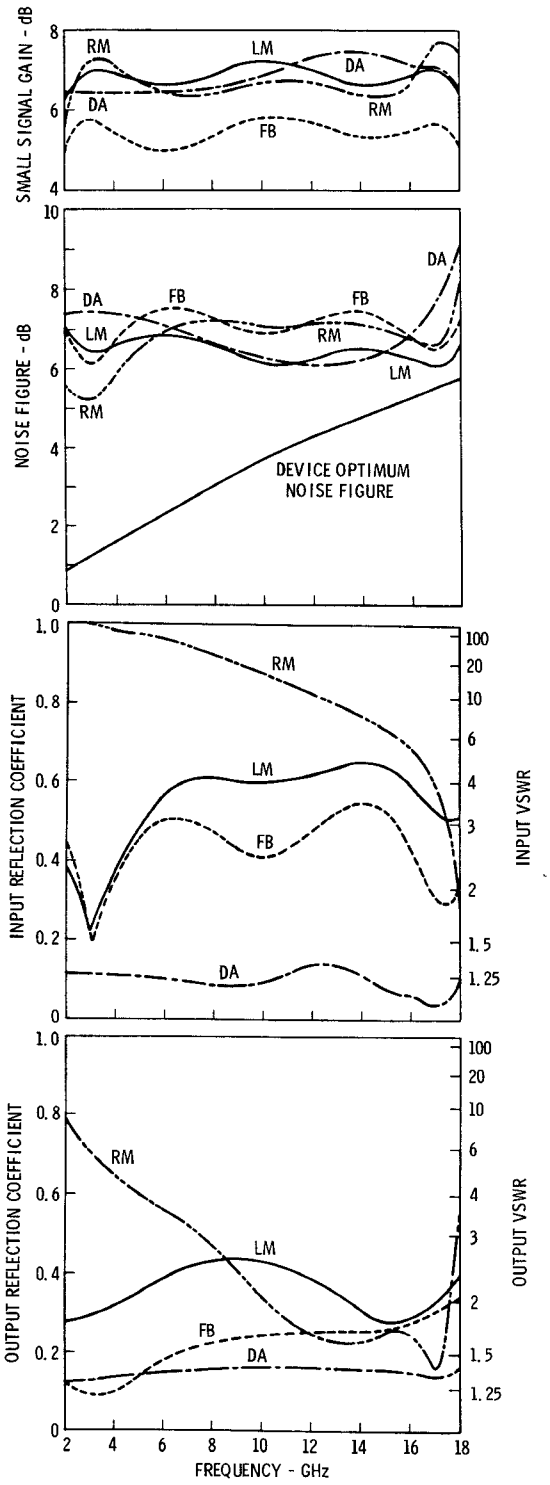

Fig. 4. Computed performance characteristics of the 2–18-GHz amplifier types employing the active device of Fig. 1.

acceptable up to three stages, as long as gain flatness is of concern only the distributed amplifier principle appears to be usable above three stages. The data in Table II clearly demonstrates the distributed amplifier's superior input and output match performance, making it the logical choice for most high-gain 2–18-GHz applications. However, any appreciable reduction of this frequency band may render the feedback or the lossy match amplifier the best suited candidate, while, for frequency bands below two octaves,

TABLE I
SINGLE-STAGE AMPLIFIER PERFORMANCE

SINGLE-ENDED AMPLIFIER PERFORMANCE						
TYPE	SS GAIN dB	NOISE FIGURE dB	MAX. VSWR		MIN. REVERSE ISOLATION dB	MIN. STABILITY FACTOR
			INPUT	OUTPUT		
RM	6.6 ± 1.0	6.7 ± 1.6	∞	7.3	-20.6	0 21
LM	6.8 ± 0.5	6.6 ± 0.5	4.7	2.6	-21.6	1 74
FB	5.4 ± 0.5	6.9 ± 0.7	3.4	2.0	-21.3	2.90
DA	7.0 ± 0.5	7.7 ± 1.5	1.3	1.4	-21.6	2.75

TABLE II
MULTISTAGE AMPLIFIER PERFORMANCE

MULTI-STAGE AMPLIFIER PERFORMANCE					
STAGES	TYPE	SS GAIN dB	MAX. VSWR		MIN K-FACT.
			INPUT	OUTPUT	
1	RM	6.6 ± 1 0	∞	7 3	0 21
	LM	6.8 ± 0 5	4.7	2 6	1.74
	FB	5.4 ± 0 5	3 4	2 0	2 80
	DA	7.0 ± 0.5	1 3	1.4	2 75
	AM	5 8 ± 0.7	2 6	2.4	6.0
2	RM	15.5 ± 5.6	–	–	-23.8
	LM	14.3 ± 1.7	6.9	2.7	5.50
	FB	11.2 ± 1.0	3.4	2.1	18 1
	DA	14.6 ± 1 0	1.5	1.6	13.5
	AM	13.8 ± 2.2	2.5	2.6	40.2
3	RM	–	–	–	–
	LM	20.9 ± 3.0	7.5	2.7	18.8
	FB	17.2 ± 1.8	3 4	2.1	108 8
	DA	21 8 ± 1.5	1.5	1 6	75 7
	AM	20.0 ± 1 5	2.6	2.8	260.0
4	RM	–	–	–	–
	LM	27.9 ± 4.6	7.6	2 7	64 6
	FB	22.7 ± 3.0	3.4	2 1	672 7
	DA	29.0 ± 2 0	1 5	1.6	408 2
	AM	27.1 ± 2.8	2.6	2.8	>1000
6	RM	–	–	–	–
	LM	43.8 ± 9.8	7.6	2.7	>1000
	FB	34 1 ± 5.0	3.4	2 1	>1000
	DA	43.5 ± 3 0	1.5	1.6	>1000
	AM	40.2 ± 6.4	2.6	2.8	>1000

the reflective match principle may survive its opponents in the competition for the best overall performance.

So far, we have determined that the best overall performance of our multistage 2–18 GHz amplifier with passive matching elements will be achieved when using the *DA* principle. However, comparing the noise figures of the modules of Fig. 2, we find from Fig. 4 that the distributed amplifier module exhibits the highest maximum noise figure. Hence, the question arises whether and how the noise characteristics can be improved without significantly impairing the other performance parameters.

A closer look at Fig. 4 reveals that the lossy match amplifier (*LM*) achieves the best overall noise performance. From this, we should expect that a modification of the *DA* module towards the *LM* module would bring about an improvement of the *DA* noise figure. Fortunately, the principle of the lossy match and the distributed amplifier are somewhat related, for, when removing the elements linking together the transistors of a distributed amplifier, it turns into a lossy match amplifier. Therefore, reducing the lengths of the linking transmission lines from those in Fig. 2 (*DA*) should improve the noise figure at the high end of the frequency band, possibly compromising the reflection coefficients and gain flatness.

It is known from the literature that the resistive components of the idle ports' terminations have their greatest

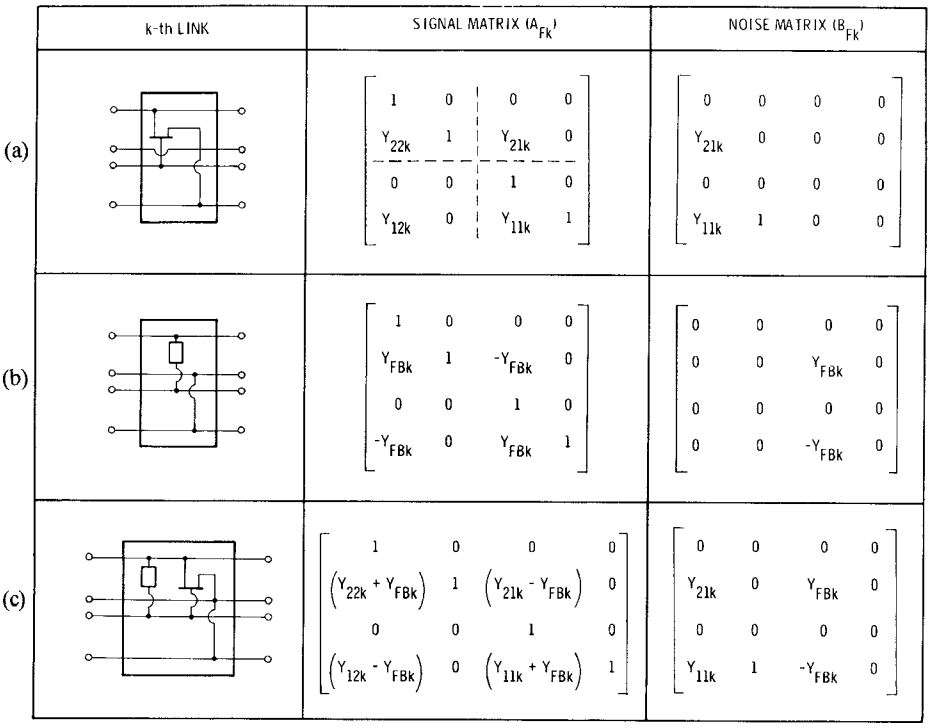

Fig. 5. Signal matrix $[A_{FK}]$ and noise matrix $[B_{FK}]$ of the distributed amplifier's basic link when employing feedback.

impact on the noise figure at the low end of the frequency band [8]. In this range, their share in the amplifier's noise figure may be reduced by partial or total elimination of these resistive components whose gain equalizing and matching functions may be performed by using negative feedback. In this case, the computation of the noise figure, the gain, and the reflection coefficients can be accomplished by using formulas published in the literature substituting, however, the signal matrix $[A_{FK}]$ and the noise matrix $[B_{FK}]$ of the active device (Fig. 5(a)) with that of the active device employing feedback (Fig. 5(c)) [8].

The circuits in Fig. 6 represent three of many combinations that are worth exploring: the distributed amplifier with complex terminations (LMDA); with negative feedback (FBDA); and with both complex terminations and negative feedback (LMFBDA). A comparison of these circuits with that of the distributed amplifier in Fig. 2 (*DA*) shows a significant reduction in the lengths of the linking transmission lines, especially in the gate line. The performance results of the modules illustrated in Fig. 6 are plotted in Fig. 7 and summarized in Table III. The maximum noise figure of the LMDA is reduced by $\Delta_{NF} = 1.4$ dB, an improvement that has been paid for by a partial deterioration of the input match and, to a lesser degree, by an increase in the gain variation. In general, the FBDA and the LMFBDA circuit do not measure up to the LMDA's overall performance and, in addition, are more complicated and, therefore, of less practical interest. Since the LMDA of Fig. 6 is identical to the DA of Fig. 2, except for the dimensions of the individual circuit elements, it emerges as the optimum choice when the noise figure is of more concern than the input match and the gain variation (Table

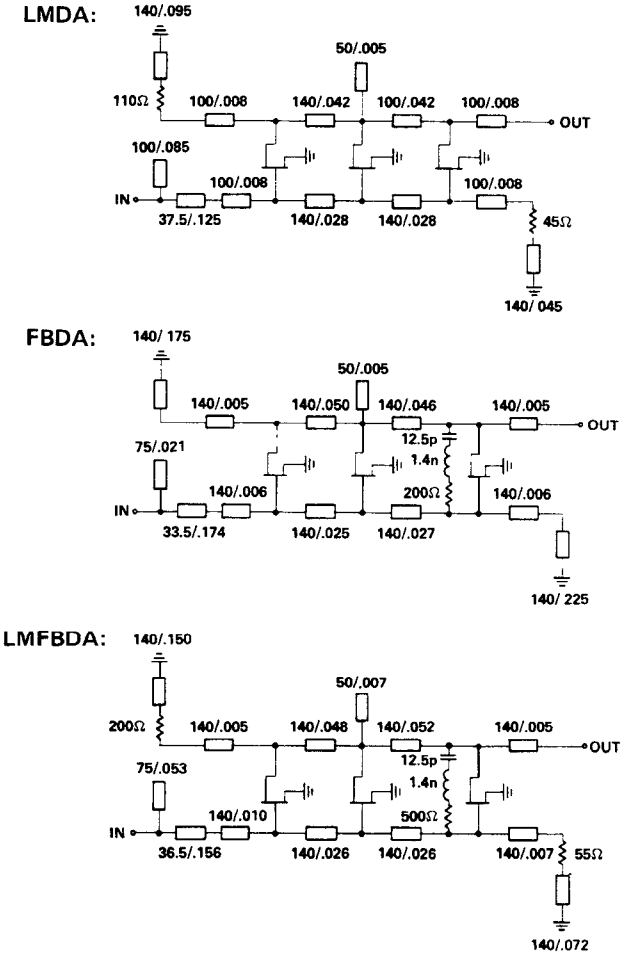

Fig. 6. Proposed distributed amplifier topologies to reduce noise figure (lengths of transmission lines in inches for air dielectric).

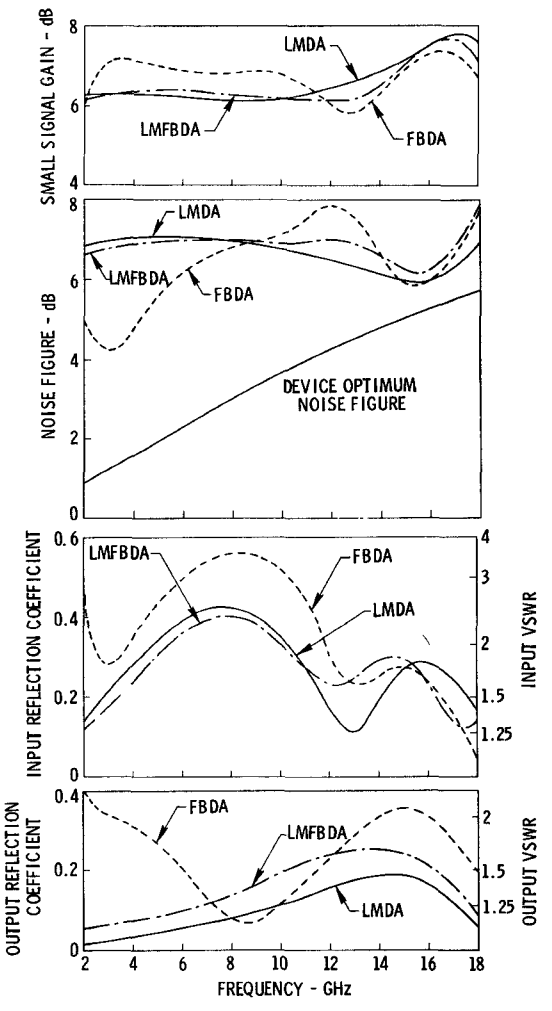

Fig. 7. Computed performance characteristics of the distributed amplifier circuits proposed in Fig. 6.

TABLE III
SUMMARY OF THE SINGLE-STAGE DISTRIBUTED AMPLIFIER CHARACTERISTICS

DISTRIBUTED AMPLIFIER PERFORMANCE				
TYPE	SS GAIN dB	NOISE FIGURE dB	MAXIMUM VSWR	
			INPUT	OUTPUT
LMDA	7.0 ± 0.8	6.5 ± 0.6	2.5	1.5
FBDA	6.6 ± 0.8	6.1 ± 1.9	3.5	2.3
LMFBDA	6.9 ± 0.8	7.0 ± 0.9	2.3	1.7

TABLE IV
SUMMARY OF THE MULTISTAGE DISTRIBUTED AMPLIFIER CHARACTERISTICS

LMDA – MULTISTAGE AMPLIFIER PERFORMANCE			
STAGES	SS GAIN dB	MAXIMUM VSWR	
		INPUT	OUTPUT
1	7.0 ± 0.8	2.5	1.5
2	14.0 ± 1.4	2.6	1.4
3	21.0 ± 2.1	2.7	1.4
4	28.0 ± 2.8	2.6	1.4
6	41.9 ± 4.2	2.6	1.4

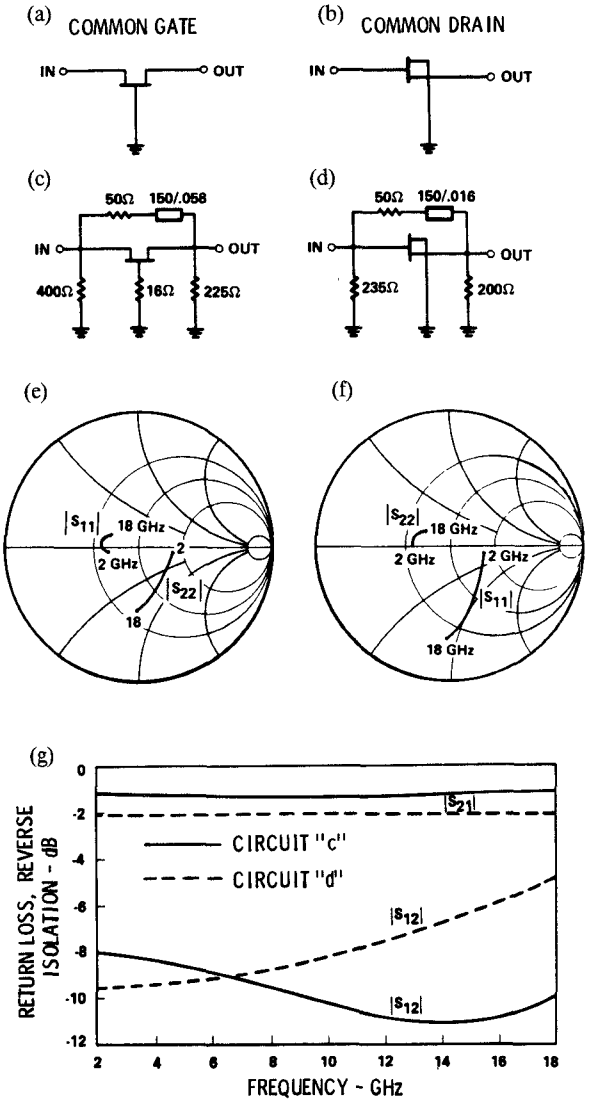

Fig. 8. Common-gate input stage and common-drain output stage (lengths of transmission lines in inches for air dielectric).

IV). A comparison of the LM circuit's performance in Fig. 4 with that of the LMDA circuit in Fig. 7 reveals identical maximum noise figures and a somewhat better gain flatness of the *LM* module. However, the LMDA circuit clearly exhibits, by far, the better input and output VSWR's, making it more suitable for multistage operation. In the final analysis, the specifications of the amplifier will dictate which approach to take unless added complexity or other reasons rule out the expenditure for a lower noise figure.

B. Matching with Active Elements

In the preceding part, we have compared a class of amplifiers whose ports are matched to a 50-Ω system by means of networks that exclusively consist of passive elements, i.e., components that are not capable of amplifying a signal. In the following, we will briefly discuss a group of amplifiers employing active elements, namely MESFET's, which are able to accomplish the same task, i.e., provide acceptable input and output impedances. This class of

amplifiers, which has recently found its way into the design of microwave solid-state amplifiers, may be collectively described as active-match amplifiers [9]–[13].

It is well known that a GaAs MESFET operated in "common-gate" configuration as shown in Fig. 8(a) is capable of providing a good input match. The significance of the common-gate input circuit can be easily understood by examining its scattering parameters. To make matters simple, we determine the S-parameters for those frequencies for which the MESFET's parasitics are negligible and, in addition, neglect all resistive elements except for the drain source conductance G_{ds}. For a source impedance of Z_1 and a load impedance of Z_2, we find

$$S_{11} = \frac{1 - g_m Z_1 + G_{ds}(Z_2 - Z_1)}{1 + g_m Z_1 + G_{ds}(Z_2 + Z_1)} \tag{4a}$$

$$S_{12} = \frac{2G_{ds}\sqrt{Z_1 Z_2}}{1 + g_m Z_1 + G_{ds}(Z_2 + Z_1)} \tag{4b}$$

$$S_{21} = \frac{2(g_m + G_{ds})\sqrt{Z_1 Z_2}}{1 + g_m Z_1 + G_{ds}(Z_2 + Z_1)} \tag{4c}$$

$$S_{22} = \frac{1 + g_m Z_1 - G_{ds}(Z_2 - Z_1)}{1 + g_m Z_1 + G_{ds}(Z_2 + Z_1)}. \tag{4d}$$

It can be easily seen from (4) that, for $g_m Z_1 = 1 + G_{ds}(Z_2 - Z_1)$, the input reflection coefficient becomes $|S_{11}| = 0$ and the associated gain is $G = |S_{21}|^2 = Z_2/Z_1$, i.e., 0 dB for $Z_1 = Z_2 = Z_0$. Under the condition that $R_{ds} \gg Z_2 + Z_1$, the output reflection coefficient approaches $|S_{22}| = 1$. Thus, a tradeoff exists between the input match on one hand and the gain and the output match on the other. For the practical device characterized in Fig. 1 and $Z_1 = Z_2 = Z_0$, the maximum magnitudes of the reflection coefficients are $|S_{11}| = 0.138$ and $|S_{22}| = 1.36$ between 2 and 18 GHz which compares to $|S_{11}| = 0.145$ and $|S_{22}| = 0.87$, respectively, when calculated with (4a) and (4d). Furthermore, the approximations of (4) which yield acceptable magnitudes of the scattering parameters up to 4 GHz are independent of frequency and therefore do not reflect the frequency dependence of the scattering parameters' phase angles. Over the 2–18-GHz band, these angles vary between $-109° \geqslant \angle S_{11} \geqslant -179°$, $-4° \geqslant \angle S_{22} \geqslant -69°$ and $-7° \geqslant \angle S_{21} \geqslant -89°$, a fact that has to be taken into account in the design of the active match input stage.

A similar situation exists for the device in "common-drain" configuration, only the roles of the ports are reversed, as can be easily seen from the low-frequency S-parameters

$$S_{11} = 1 \tag{5a}$$

$$S_{12} = 0 \tag{5b}$$

$$S_{21} = \frac{2g_m\sqrt{Z_1 Z_2}}{1 + (g_m + G_{ds})Z_2} \tag{5c}$$

$$S_{22} = \frac{1 - (g_m + G_{ds})Z_2}{1 + (g_m + G_{ds})Z_2}. \tag{5d}$$

In the absence of parasitics, the input terminal presents an open circuit and the input and the output are totally isolated from each other. For $(g_m + G_{ds})Z_2 = 1$, the output reflection coefficient becomes $|S_{22}| = 0$ while the gain is $G = |S_{21}|^2 = g_m^2 Z_1 Z_2$, i.e., $G \geqslant 0$ dB when $g_m \geqslant 20$ mS and $Z_1 = Z_2 = Z_0$. Comparing the magnitudes of the reflection coefficients computed for the device of Fig. 1 with those calculated with (5), we find $1 \leqslant |S_{11}| \leqslant 1.27$ versus $|S_{11}| = 1$ and $0.218 \leqslant |S_{22}| \leqslant 0.233$ versus $|S_{22}| = 0.226$ when $Z_1 = Z_2 = Z_0$. As was the case for the common-gate configuration, the phase angles of the practical device vary significantly from the constant angles determined with (5) over the 2–18-GHz frequency range.

At this point, a brief discussion on the influence of the source and load impedance of the common-gate FET (CGF) and the common-drain FET (CDF) on their individual S-parameters is in order. As can be seen from (4) and (5), the choices of Z_1 and Z_2 have an appreciable impact on the gain and the reflection coefficients of both FET configurations, and this is true for the common-source FET (CSF) as well. For a demonstration, let us assume we cascade three idealized devices characterized by $g_m = 20$ mS and $R_{ds} = 272\ \Omega$ ($G_{ds} = 3.68$ mS) in accordance with the simple active match amplifier circuit of Fig. 9. Choosing $R_1 = 160$ and $R_2 = 750\ \Omega$, the three-stage amplifier's computed gain is $G = 14.0$ dB and the computed maximum VSWR's are 1.34:1 for the input and 1.18:1 for the output port. As in all of our studies, the source and load impedance of the amplifier are $Z_0 = 50\ \Omega$. For comparison, the idealized versions of the individual devices when operating in a 50-Ω system yield gains of $G = 0$ dB for the CGF, $G = 4.55$ dB for the CSF, and $G = -0.76$ dB for the CDF module. The computed parameters above are independent of frequency due to the choice of the device model. As one might expect, the technique of providing a set of source and load impedances over multi-octave bands loses its strength at frequencies where the parasitics of the actual device exert a strong influence on the S-parameters. When replacing the idealized model with the transistor of Fig. 1, and choosing $R_1 = 125$ and $R_2 = 400\ \Omega$, our three-stage amplifier's gain deteriorates from $G = 14.1$ dB at 2 GHz to $G = 5.8$ dB at 7 GHz. However, across the same frequency band, the maximum input and output VSWR's do not exceed 1.4:1 and 1.5:1, respectively. Of course, there are means of extending the band coverage by introducing additional circuit elements. However, it appears rather difficult to extract appreciable gain and simultaneously achieve superior matching from either the CGF or the CDF module when the frequency band is 2–18 GHz, unless we succeed in significantly reducing the parasitics of our devices.

While as we have demonstrated, the common-gate FET (CGF) serves as a good input match and the common-drain FET (CDF) as a good output match, the CGF output port and the CDF input port present unacceptable and, over the upper part of the frequency band, often negative impedances to the amplifying section to be placed between them. Shunt resistors, as well as parallel and series feedback, may

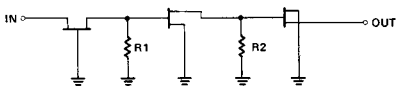

Fig. 9. Simple active match amplifier circuit.

be used to improve the reflection coefficients of the ports facing the actual amplifier section and simultaneously provide unconditional stability for both active matching circuits. The schematics of the circuits which result from such stabilizing techniques when employing the device of Fig. 1 are shown in Fig. 8(c) and 8(d), while the curves of the circuits' reflection coefficients are plotted in Fig. 8(e) and 8(f). Finally, the loss and reverse isolation of both networks are shown in Fig. 8(g). The results presented have been computed for a source and load impedance of $Z_1 = Z_2 = 50\ \Omega$. The common-gate circuit of Fig. 8(c) produces a flat gain response and an acceptable input VSWR brought about by the use of the parallel and the series ohmic feedback, as well as the lossy shunts. However, the noise figure is impaired, primarily due to the noise injected by the series feedback resistor. The elimination of the latter is therefore beneficial for low-noise operation.

Since in many practical cases the output match of the last amplifier stage needs little improvement, an active match output may not be needed or not be able to provide any appreciable improvement, especially over multi-octave bandwidths. The schematic of an active match amplifier module that employs the device of Fig. 1 in both the active-match input stage and the subsequent amplifier stage is shown in Fig. 10(a), while Fig. 10(b) represents the gain, the noise figure, and the reflection coefficients of this module between 2 and 18 GHz. For reasons of lower noise figures, we have not made use of the series feedback, even though this measure accounted for a deteriorated input match. The amplifier stage is of the lossy match type and, because of it, has an acceptable output VSWR. The input VSWR shows significant improvement (2.6:1) over the lossy match module of Fig. 2 (4.7:1). However, a comparison of Fig. 10(b) and Fig. 4 reveals a ± 0.7-dB gain variation and a 9.6-dB maximum noise figure of the active match amplifier versus a ± 0.5-dB gain variation and a 7.1-dB maximum noise figure of the lossy match module. The output VSWR's are 2.4:1 for the AM unit and 2.6:1 for the LM unit. Replacing the common-gate input stage of Fig. 10 with that of Fig. 8(c) and, in addition, optimizing the second stage for gain results in an improved input VSWR (2.0:1) and similar gain performance (6.0 ± 0.75 dB). However, the maximum noise figure increases from 9.6 to 13.0 dB, primarily due to the noise contributed by the series feedback resistor.

The element values of the module shown in Fig. 10(a) need to be reoptimized in order to achieve an acceptable gain performance when more than one LM gain stage follows the active match input stage. The characteristics of multistage amplifiers consisting of n LM gain stages preceded by an AM input stage are also summarized in Table II. The results presented are based on element values

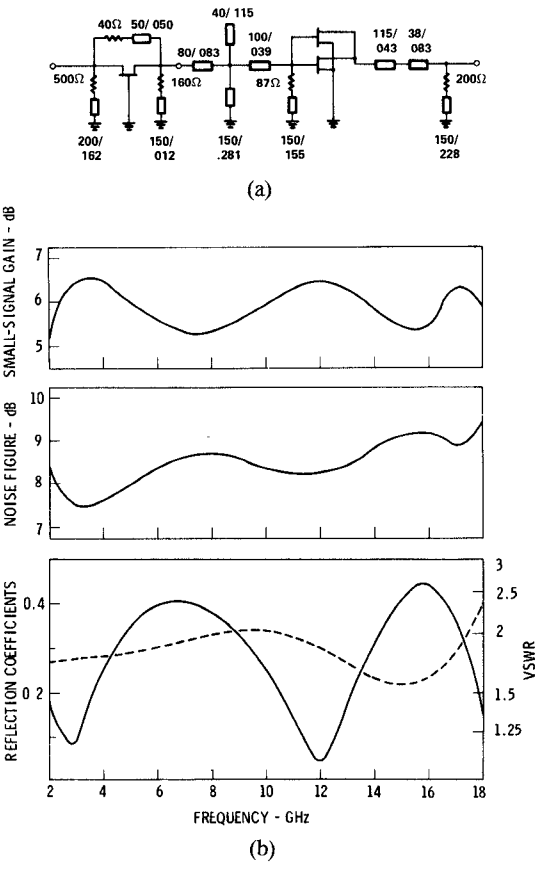

Fig. 10. (a) Active match amplifier schematic and (b) performance (—— input, ---- output refl. coeff.)

obtained from the optimization of the three-stage unit ($n = 3$). The data reveals that our active match amplifier incorporating n stages has a gain performance similar to that of the LM amplifier with significantly improved input VSWR and comparable output VSWR. Furthermore, a better gain flatness is obtained for $n > 2$. However, as were the LM and FB amplifiers, it is not a serious competitor to the distributed amplifier in the 2–18-GHz frequency band when using the device of Fig. 1. In addition, biasing the common-gate input stage via the lossy match networks on either side of the transistor results in significant voltage drops and efficiency losses.

III. Experimental Results

In the preceding chapter, we have concentrated our efforts on discussing the designs of multistage 2–18-GHz amplifiers and have compared their computed performances. Now we will attempt to assemble some of the supporting experimental results.

A. Previously Reported Data

A number of multi-octave single-ended solid-state amplifiers employing lossy match, feedback, distributed, and active match circuits have been described in the literature [6]–[30]. While the frequency coverage of the first three amplifier types has been extended into Ku-band and, in case of the distributed amplifier, beyond 18 GHz, the

design efforts of the active match amplifiers have almost exclusively been confined to frequencies below 5 GHz, with one known exception [13].

Until now, no data has come to our attention on the successful design of a practical 2–18-GHz reflective match amplifier. On the other hand, H. Q. Tserng and co-workers have reported small-signal gains of $G = 6.4 \pm 1.0$ dB from 3.2 to 18 GHz in a single-ended module designed for 6–18-GHz operation [14]. From 3 to 2 GHz, this module's gain increased rather rapidly to $G > 10$ dB; yet, when driven with $P_{in} = 20$ dBm, a less varying gain of $G = 5 \pm 2.3$ dB was observed between 2 and 18 GHz.

A. M. Pavio demonstrated for the first time the feasibility of a 2–18-GHz feedback amplifier and was able to achieve $G = 11.0 \pm 2.1$ dB across this band, as well as $G = 14.4 \pm 2.6$ dB from 2.8 to 18 GHz after self-biasing was added [15]. Since feedback amplifiers, even at low frequencies, can be realized on very small substrates, they offer an economical design option to monolithic technology. P. A. Terzian *et al.* measured a small-signal gain of $G = 6.0 \pm 0.2$ dB between 1 and 7 GHz in a monolithic feedback amplifier using lumped elements [16]. The input and output VSWR were 2.3:1 and 1.7:1, respectively. In a similar approach, W. O. Camp *et al.* realized $G = 7.0 \pm 0.7$ dB on a 0.76-mm^2 GaAs chip with a maximum input VSWR of 3.6:1 and a maximum output VSWR of 2.4:1 [17]. R. N. Rigby and co-workers achieved $G = 5.8 \pm 0.6$ dB between 0.6 and 6.1 GHz, realizing maximum VSWR's of 3.2:1 for the input and 2:1 for the output port [18]. K. Honjo *et al.* reported on a two-stage monolithic amplifier using negative feedback and self-biasing for the second stage [19]. The authors achieved a 3-dB bandwidth gain of $G = 13.5$ dB from 500 kHz to 2.8 GHz. The unit exhibited an input VSWR of $\leqslant 2.5:1$ from 500 kHz to 2.1 GHz and an output VSWR of $\leqslant 1.6:1$ between 500 kHz and 4.5 GHz.

The concept of the lossy match solid-state amplifier at microwave frequencies was studied by two teams. In France, T. Obregon *et al.* demonstrated $G = 12.0 \pm 2.1$ dB in a self-biased three-stage unit operating between 150 MHz and 16 GHz, and measured a maximum noise figure of $NF = 8.5$ dB from 1–12.4 GHz [20]. At almost the same time, K. Honjo and Y. Takayama in Japan obtained an 8.6-dB gain over the 3-dB bandwidth from 800 kHz to 9.5 GHz [21]. The input VSWR was better than 4:1 over the 1 MHz to 10-GHz frequency range, while a 2:1 VSWR was obtained between 2 MHz and 9 GHz. The amplifier had an output power at 1-dB gain compression of 12 dBm over the 2 MHz to 9-GHz range. A maximum noise figure of 8 dB was observed from 50 MHz to 6 GHz. The widest band coverage reported in a lossy match amplifier was achieved by M. Mamodaly and co-workers, who were able to obtain $G = 4.5 \pm 1.5$ dB in a 100 MHz to 17 GHz two-stage amplifier with gain control by way of dual-gate GaAs MESFET's [22]. Maximum input and output VSWR's were 3.5:1 and 2.5:1, respectively, and the unit's gain could be varied by 15 dB.

Concerning distributed amplifiers, Y. Ayasli *et al.* succeeded in realizing $G = 11.6 \pm 1.6$ dB in 2–20-GHz two-stage monolithic amplifiers on $2.2 \times 5.5 \times 0.1$ mm GaAs substrates [23]. The same team was successful in combining the powers of two distributed amplifiers by devising a unique circuit that consists of two distributed amplifiers sharing a common drain line [24]. The amplifier which uses a power divider to feed two input ports produced a nominal output power of 250 mW at an input power of 20 dBm from 2–18 GHz.

The activities in the field of active-match amplifiers have mostly been concentrated at frequencies below 5 GHz. The only exception known to this author is the work done by W. C. Peterson *et al.* who reported on a 0.1–10.0-GHz monolithic four-stage amplifier design consisting of a common-gate active match input stage, two common-source lossy match amplifier stages, and a common-drain output stage [13]. Manufactured on a 2.5-mm^2 chip, the amplifier yielded $G = 7.2 \pm 1.2$ dB of small-signal gain between 0.7 and 9.0 GHz. The input and output reflection coefficients over this band were better than 2:1. In contrast, at lower frequencies, where the stability of the circuits can more easily be obtained, a number of researchers have made use of active matching. In 1978, R. L. Van Tuyl first described his monolithic integrated 4-GHz amplifier [9]. This unit went far beyond the concept of active matching, for Van Tuyl replaced passive with active elements throughout the amplifier. While a common-drain circuit was employed as the output stage, the resistor, normally used in parallel feedback, was replaced by a MESFET. Furthermore, the resistive load had given way to an active load in order to improve the unit's large-signal performance. As the basic amplifying element, a common-source MESFET was employed and biasing of this direct coupled amplifier was accomplished by means of level shifting diodes. Thus, a single amplifier stage used five FET functions. Many refinements have altered this circuit type in subsequent years, among them a resistively loaded common-gate input stage [10], [11]. A typical voltage gain of 26 dB between 5 MHz and 3.3 GHz with less than 1.3:1 of input VSWR have been achieved in a 0.4×0.65 mm gain block incorporating 17 MESFET's. Using the circuit techniques described by R. L. Van Tuyl, D. P. Hornbuckle, and D. B. Estreich, a nominal gain of $G = 20$ dB, as well as an input and output VSWR of 1.5:1 and 2:1, respectively, were measured by V. Pauker and M. Binet in their 0.11–3.2-GHz amplifier. However, in their unit the feedback was performed by a resistor [12].

B. Recent Experimental Data

In this section, we shall add some of our own experimental data recently obtained from a 3–17.5-GHz reflective match module, a two-stage and a four-stage 2–18-GHz feedback amplifier, as well as a two-stage and a four-stage 2–18-GHz distributed amplifier. While the results support what has been discussed in Section II, they are not meant to represent the experimental proof to the computed results of the circuits in Fig. 2. In particular, the *RM* module was intended to operate in the 4–18-GHz band, while the *FB* amplifiers were designed for a single GaAs MESFET capa-

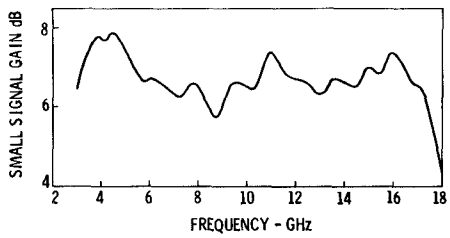

Fig. 11. Measured gain of a 3–17.5-GHz reflective match gain module.

ble of replacing the two parallel devices shown in the schematic of Fig. 2 (*FB*) and described in Fig. 1. However, except for the distributed amplifier's biasing circuitry, the types of the passive elements and their locations are identical to those shown in the schematics of Fig. 2. Only their values have been altered in order to satisfy specific requirements.

1) Reflective Match Amplifier: While no attempt was made to design a 2–18-GHz reflective match amplifier, we have studied the feasibility of a 4–18-GHz module using the GaAs MESFET described in Fig. 1. The rather limited effort was confined to the design of a single-stage module and was terminated with the measurements of its gain and reflection coefficients. The gain performance is plotted in Fig. 11, demonstrating $G = 6.8 \pm 1.1$ between 3 and 17.5 GHz. The measured reflection coefficients range from a maximum of $|S_{11}| = 0.99$ and $|S_{22}| = 0.89$ at 3 GHz to a minimum of $|S_{11}| = 0.33$ and $|S_{22}| = 0.20$ at 18 GHz. Obviously, the extremely high reflection coefficients at the low end of the frequency band and the necessity of using tandem couplers due to the multi-octave bandwidth make it quite a challenge to realize a reliable 2–18-GHz *RM* amplifier performance and therefore invite the consideration of alternate approaches.

2) Feedback Amplifier: Encouraged by the computed results shown in Fig. 4 and the multi-stage characteristics of Table II, it was decided to study the feasibility of a two-stage and a four-stage feedback amplifier. Since, however, the use of two parallel transistors in a feedback amplifier is somewhat impractical, the decision was made to replace the two devices with a single sub half-micron gate GaAs MESFET of matching characteristics. The element values of its equivalent circuit are presented in Table V. Except for the short-circuited shunt element of the input matching network, which was omitted, all stages are characterized by the schematic in Fig. 2 (*FB*) and connected by a T-shaped interstage matching circuit consisting of an open-circuited shunt stub flanked by transmission lines on both sides. In contrast to the circuit diagram of Fig. 2 (*FB*), the actual amplifiers incorporated the following resistors: $R_G = 475\ \Omega$, $R_D = 220\ \Omega$, $R_{FB1} = 240\ \Omega$, $R_{FB2} = 500\ \Omega$ in case of the two-stage unit and $R_G = 475\ \Omega$, $R_D = 235\ \Omega$, $R_{FB1} = 200\ \Omega$, $R_{FB2} = R_{FB3} = R_{FB4} = 500\ \Omega$ for the four-stage unit. The overall dimensions of the two circuits are $0.308 \times 0.120 \times 0.015$ in and $0.530 \times 0.120 \times 0.015$ in, respectively. Alumina was used as substrate material.

TABLE V
ELEMENT VALUES OF THE SUB HALF-MICRON GATE GaAs MESFET

INTRINSIC ELEMENTS		EXTRINSIC ELEMENTS	
gm	= 53 mS	R_g	= 2 ohm
τ_o	= 3.2 psec	L_g	= .097 nH
C_{gs}	= .345 pF	R_s	= .95 ohm
C_{gd}	= .035 pF	L_s	= .016 nH
C_{dc}	= .011 pF	C_{ds}	= .115 pF
R_{gs}	= 4.7 ohm	R_d	= 2.2 ohm
R_{ds}	= 213 ohm	L_d	= .177 nH

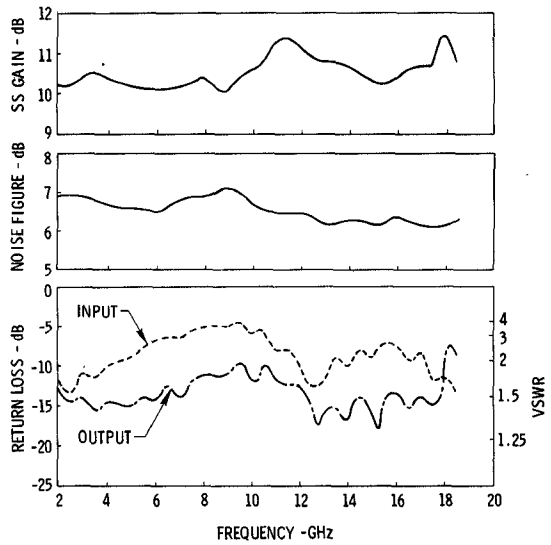

Fig. 12. Measured small-signal gain, noise figure, and return loss of the 2–18-GHz two-stage feedback amplifier.

Fig. 12 shows the curves of the small-signal gain, the noise figure, and the return loss of the two-stage amplifier between 2 and 18.5 GHz. A gain of $G = 10.8 \pm 0.7$ dB and maximum return loss of -4.4 dB (VSWR of 4:1) for the input port and -9.5 dB (VSWR of 2:1) for the output port were measured between 2 and 18 GHz. Across the same frequency band, a maximum noise figure of $NF = 7.1$ dB was recorded. The performance characteristics of the four-stage amplifier are plotted in Fig. 13 between 0.5 and 18.5 GHz. In this case, a gain of $G = 23.1 \pm 1.1$ dB and a maximum return loss of -4.0 dB (VSWR of 4.4:1) for the input port and -7.5 dB (VSWR of 2.5:1) for the output port were measured across the 18.0-GHz bandwidth. The associated maximum noise figures were $NF = 7.9$ dB from 0.5–18.5 GHz and $NF = 7.0$ dB from 2.0–18.5 GHz. As in all of our studies, the emphasis was put on gain flatness and no effort was made to improve either the noise figure or the return loss of the input or the output port. Nevertheless, the above measurements mark, to the best of our knowledge, the lowest instantaneous noise figure reported to date across the respective frequency bands. The minimum output power at the 1-dB compression points was $P_{out} = 13.5$ dBm.

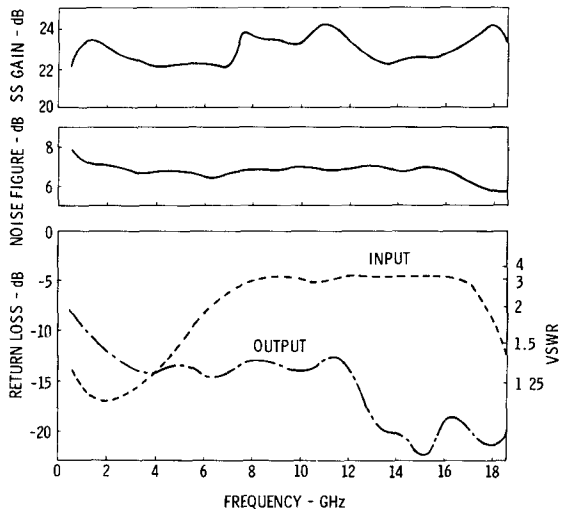

Fig. 13. Measured small-signal gain, noise figure, and return loss of the 0.5–18.5-GHz four-stage feedback amplifier.

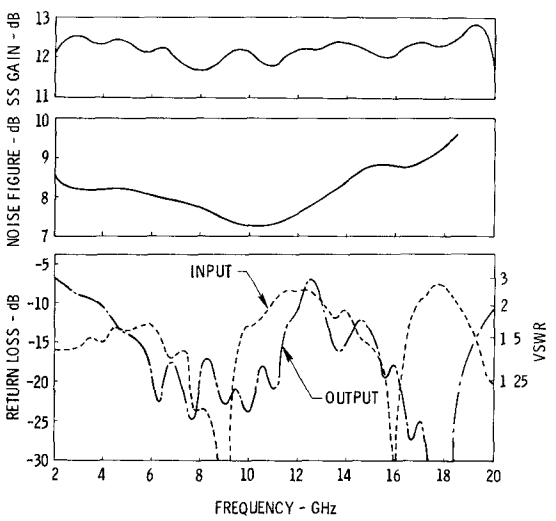

Fig. 14. Measured small-signal gain, noise figure, and return loss of the 2–18-GHz two-stage distributed amplifier.

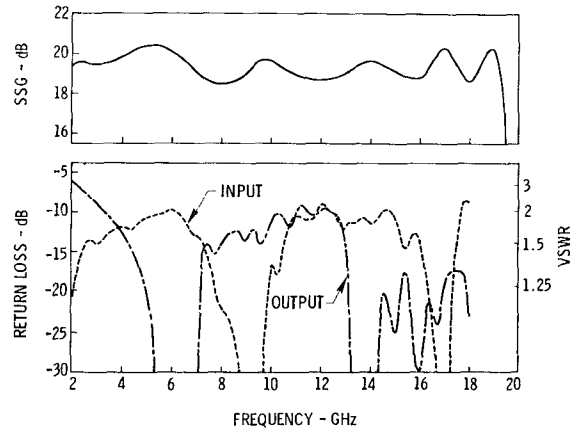

Fig. 15. Measured small-signal gain and return loss of the 2–18-GHz four-stage distributed amplifier.

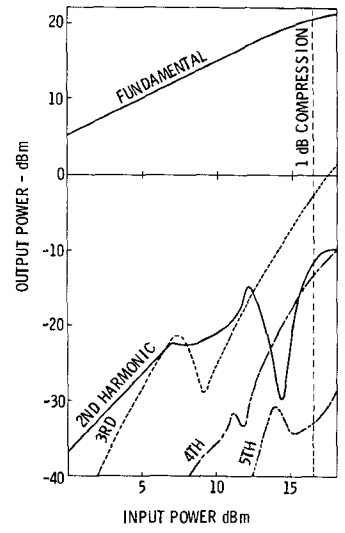

Fig. 16. Harmonic output of the single-stage 2–18-GHz distributed amplifier ($f_0 = 2$ GHz).

3) Distributed Amplifier: The data reported here was taken on a two-stage and a four-stage amplifier whose individual stages are essentially built to the schematic of Fig. 2 (*DA*), with the exception of the drain bias circuitry and the resistance of the drain termination. Since each stage operated at a drain current of approximately 120 mA, a voltage drop of 24 V would have occurred across the 200-Ω termination resulting in 2.9 W of power dissipation in the 3×12 mils tantalum nitride resistor. To avoid a decrease in reliability due to overheating and a loss in efficiency, we chose to bias the drains directly through a high-impedance short-circuited shunt stub located parallel to the termination resistor. The latter was changed from 200 to 125 Ω for best gain flatness. The fabrication and dimensions of the modules have been described elsewhere [7].

The gain, the noise figure, and the return loss of the two-stage unit are plotted in Fig. 14. A gain of $G = 12.3 \pm 0.55$ dB and a maximum return loss of -8 dB (VSWR of 2.3:1) for the input and -7 dB (VSWR of 2.6:1) for the output terminal were measured from 2.0–20.0 GHz, while the maximum noise figure was $NF = 9.6$ dB between 2 and 18 GHz. The curves for gain and return loss of the four-stage amplifier are shown in Fig. 15. This unit exhibits a gain of $G = 19.4 \pm .9$ dB, while a maximum input return loss of -7.5 dB (VSWR of 2.5:1) and output return loss of -6 dB (VSWR of 3.0:1) were achieved between 2.0 and 18.0 GHz. Across the same band, a maximum noise figure of $NF = 11$ dB was measured. It should be reemphasized that both amplifiers were tuned for best gain flatness, compromising noise figure as well as optimum gain performance. Thus far, no attempt has been made to improve the noise figure by implementing the theoretical findings discussed earlier. Finally, Fig. 16 represents the harmonic output power curves of a single-stage module when driven by an input signal of $f = 2$ GHz at various power levels. They show a 23-dB separation between fundamental and the dominant harmonic output power at the 1-dB compression point.

IV. Conclusion

The computed performance characteristics of the reflective match, the lossy match, the feedback, the distributed, and the active match amplifier have been compared across the 2–18-GHz frequency band. In addition, a set of formulas has been developed that demonstrates the significant interdependence of an amplifier's gain and reflection coefficients when feedback, lossy matches, or both are being employed. When utilizing one and the same type of active device in all five circuit types, the computed results reveal gain characteristics that make it difficult to favor one concept over the others. However, when the gain specifications require the cascading of two or more gain modules, as is the case in most practical applications, the reflection coefficients of the input and output ports become of major significance and the choices narrow down with the number of cascaded stages. As demonstrated in Table II, for more than three stages, the distributed amplifier principle is clearly the favorite option. However, one should be quick to point out that matters are not as clear-cut when reducing the bandwidth requirement at the high end of the frequency range.

In search for a solution to improve the noise figure of the distributed amplifier for a given transistor, it was found that any improvement in noise figure impairs the amplifier's gain flatness. Of the three proposed circuit configurations discussed, that of the lossy match distributed amplifier (LMDA) appears to be the most practical solution with the best prospects in noise reduction.

In order to provide an overview of the accomplishments in the field of single-ended amplifiers, some of the previously reported data has been briefly reviewed. In addition, new test results have been presented in support of the computed data. Of the amplifiers tested recently, the reflective match gain module exhibited 6.8 ± 1.1 dB of small-signal gain from 3–17.5 GHz. However, cascading of single-ended modules was not attempted for reasons of instability. A gain of $G = 10.8 \pm 0.7$ dB and a maximum noise figure of $NF = 7.1$ dB were demonstrated in the two-stage feedback amplifier employing lossy match biasing networks. A four-stage feedback amplifier operated between 0.5 and 18.5-GHz exhibited $G = 23.1 \pm 1.1$ dB of small-signal gain and 7.9 dB of maximum noise figure. Above noise figures, though not optimized, are believed to represent state-of-the-art performance in the 2–18.5-GHz and 0.5–18.5-GHz frequency bands. The gain and the maximum noise figure measured in the two-stage distributed amplifier were $G = 12.3 \pm 0.55$ dB and $NF = 9.6$ dB, respectively. A maximum return loss of -7 dB was recorded in this direct-biased unit. With the four-stage distributed amplifier, we were able to demonstrate 19.4 ± 0.9 dB of gain and 11.0 dB of maximum noise figure. Higher order harmonic output power of a single gain module did not exceed -23 dBc up to the 1-dB compression point for a $f = 2$ GHz fundamental input signal.

In conclusion, we have found that the optimum circuit type of a GaAs MESFET amplifier depends to a great degree on the frequency band of interest, the characteristics of the active devices, and the required gain level. For the 2–18-GHz frequency band and transistors with characteristics similar to those of Fig. 1, however, the optimum multistage gain performance is offered by the distributed amplifier.

Acknowledgment

The author wishes to thank R. R. Pereira, who performed all measurements and whose skills in tuning the amplifiers greatly contributed to the success of our studies. In addition, thanks go to J. Martin and M. Lozada, who assembled the circuits. The author is indebted to W. T. Wilser, who kindly edited the manuscript, and to R. Perry, who typed the formulas. Special thanks are due to B. A. Tucker, who modified the existing computer program to include the noise contributed by feedback as expressed by the matrices of Fig. 5. Finally, the author would like to express his appreciation for the constant support and encouragement afforded by W. K. Kennedy during the course of this work.

References

[1] R. S. Engelbrecht and K. A. Kurakawa, "A wideband low noise *L*-band balanced transistor amplifier," *Proc. IEEE*, vol. 53, pp. 237–247, Mar. 1965.

[2] J. Lange, "Interdigitade stripline quadrature hybrid," *IEEE Trans. Microwave Tech.*, vol. MTT-17, pp. 1150–1151, Dec. 1969.

[3] J. P. Shelton and J. A. Mosko, "Synthesis and design of wideband equal ripple TEM directional couplers and fixed phase-shifters," *IEEE Trans. Microwave Theory Tech.*, vol. MTT-14, pp. 462–473, Oct. 1966.

[4] Y. Tajima and S. Kamihashi, "Multi-conductor couplers," *IEEE Trans. Microwave Theory Tech.*, vol. MTT-26, pp. 795–801, Oct. 1978.

[5] K. B. Niclas and R. R. Pereira, "Feedback applied to balanced FET amps," *Microwave Syst. News*, pp. 66–69, Nov. 1980.

[6] K. B. Niclas, "On design and performance of lossy match GaAs MESFET amplifiers," *IEEE Trans. Microwave Theory Tech.*, vol. MTT-30, pp. 1900–1907, Nov. 1982.

[7] K. B. Niclas, W. T. Wilser, R. T. Kritzer, and R. R. Pereira, "On theory and performance of solid-state microwave distributed amplifiers," *IEEE Trans. Microwave Theory Tech.*, vol. MTT-31, pp. 447–456, June 1983.

[8] K. B. Niclas and B. A. Tucker, "On noise in distributed amplifiers at microwave frequencies," *IEEE Trans. Microwave Theory Tech.*, vol. MTT-31, pp. 661–668, Aug. 1983.

[9] R. L. Van Tuyl, "A monolithic integrated 4-GHz amplifier," *1978 ISSCC, Dig. Tech. Pap.*, pp. 72–73, Feb. 1978.

[10] D. Hornbuckle and R. L. Van Tuyl, "Monolithic GaAs direct coupled amplifiers," *IEEE Trans. Electron Devices*, vol. ED-28, pp. 175–182, Feb. 1981.

[11] D. B. Estreich, "A wideband monolithic GaAs IC amplifier," *1982 ISSCC, Dig. Tech. Papers*, Feb. 1982, pp. 194–195.

[12] V. Pauker and M. Binet, "Wideband high gain small size monolithic GaAs FET amplifiers," *1983 Microwave Symp. Dig.*, June 1983, pp. 81–84.

[13] W. C. Petersen, D. R. Decker, A. K. Gupta, J. Dully, and D. R. Chen, "A monolithic GaAs 0.1 to 10 GHz amplifier," *1981 Microwave Symp. Dig.*, June 1981, pp. 354–355.

[14] H. Q. Tserng, S. R. Nelson, and H. M. Macksey, "2–18 GHz, high efficiency, medium-power GaAs FET amplifiers," *1981 Microwave Symp. Dig.*, June 1981, pp. 31–33.

[15] A. M. Pavio, "A network modeling and design method for a 2–18 GHz feedback amplifier," *1982 Int. Microwave Symp. Dig.*, June 1982, pp. 162–165.

[16] P. A. Terzian, D. B. Clark, and R. W. Waugh, "Broadband GaAs monolithic amplifier using negative feedback," *IEEE Trans. Microwave Theory Tech.*, vol. MTT-30, pp. 2017–2020, Nov. 1982.

[17] W. O. Camp, Jr., S. Tiwari, and D. Parsons, "2–6 GHz monolithic microwave amplifier," *1983 Microwave Symp. Dig.*, June 1983, pp 76–80.

[18] P. N. Rigby, J. R. Suffolk, and R. S. Pengelly, "Broadband monolithic low-noise feedback amplifiers," *1983 Microwave Symp. Dig.*, June 1983, pp. 41–45.
[19] K. Honjo, T. Sugiura, and H. Itoh, "Ultra-broadband GaAs monolithic amplifier," *IEEE Trans. Microwave Theory Tech.*, vol. MTT-30, pp. 1027–1033, July 1982.
[20] T. Obregon and R. Funk, "A 150 MHz–16 GHz FET amplifier," *1981 ISSCC, Dig. Tech. Papers*, Feb. 1981.
[21] K. Honjo and Y. Takayama, "GaAs FET ultrabroad-band amplifiers for Gbit/s data rate systems," *IEEE Trans. Microwave Theory Tech.*, vol. MTT-29, pp. 629–636, July 1981.
[22] M. Mamodaly, P. Quentin, P. Dueme, and J. Obregon, "100 MHz to 17 GHz dual gate variable gain amplifier," *IEEE Trans. Microwave Theory and Tech.*, vol. MTT-30, pp. 918–919, June 1982.
[23] Y. A. Ayasli, L. D. Reynolds, J. L. Vorhaus, and L. Hanes, "Monolithic 2–20 GHz GaAs traveling wave amplifier," *Electron. Lett.*, vol. 18, pp. 596–598, July 1982.
[24] Y. Ayasli, L. D. Reynolds, R. L. Mozzi, J. L. Vorhaus, and L. K. Hanes, "2–20 GHz GaAs traveling-wave power amplifier," *1983 MTT Monolithic Circuits Symp. Dig.*, June 1983, pp. 67–70.
[25] E. Ulrich, "Use of negative feedback to slash wideband VSWR," *Microwaves*, pp. 66–70, Oct. 1978.
[26] K. B. Niclas, W. T. Wilser, R. B. Gold, and W. R. Hitchens, "The matched feedback amplifier: Ultrawide-band microwave amplification with GaAs MESFETs," *IEEE Trans. Microwave Theory Tech.*, vol. MTT-28, pp. 285–294, Apr. 1980.
[27] E. L. Ginzton, W. R. Hewlett, J. H. Jasberg, and J. D. Noe, "Distributed amplifier," in *Proc. IRE*, vol. 36, Aug. 1948, pp. 956–969.
[28] Y. Ayasli, R. L. Mozzi, J. L. Vorhaus, L. D. Reynolds, and R. A. Pucel, "A monolithic GaAs 1-13 GHz traveling-wave amplifier," *IEEE Trans. Microwave Theory Tech.*, vol. MTT-30, pp. 976–981, July 1982.
[29] Y. Ayasli, J. L. Vorhaus, R. L. Mozzi, and L. D. Reynolds, "Monolithic GaAs traveling wave amplifier," *Electron. Lett.*, vol. 15, pp. 413–414, June 1981.
[30] E. W. Strid, K. R. Gleason, and J. Addis, "A dc-12 GHz GaAs FET distributed amplifier," *Res. Abstracts 1981 Gallium Arsenide Integrated Circuit Symp.*, Oct. 1983, p. 47.

Karl B. Niclas (M'63–SM'81) received the Dipl.—Ing. and Doctor of Engineering degrees from the Technical University of Aachen, Aachen, Germany, in 1956 and 1962, respectively.

From 1956 to 1962, he was with the Microwave Tube Laboratory at the Telefunken G.m.b.H. Tube Division, Ulm-Donau, Germany. He was engaged in research and development on ultra-low-noise and medium-power traveling-wave tubes. In 1958, he became Head of the company's Traveling-Wave Tube Section and Assistant Manager of the Microwave Tube Laboratory. From 1962 to 1963, he was associated as a Senior Project Engineer with General Electric Microwave Laboratory, Stanford, CA. His work was mainly concerned with theoretical and experimental investigations of single-reversal focused low-noise traveling-wave tube amplifiers, and resulted in the first lightweight amplifier of this type. In 1963, he joined the Technical Staff of Watkins–Johnson Company, Palo Alto, CA, and is presently Consultant to the Vice President, Devices Group. His current research efforts are primarily focused on advanced GaAs FET amplifiers, broad-band power combining techniques, and wide-band GaAs FET oscillator concepts. From 1967 to 1976, he was Manager of the company's Tube Division. Before that, he was Head of the Low-Noise Tube R & D Section, and prior to that he was engaged in a research program on new concepts for achieving high efficiency in traveling-wave tubes. He is the author of numerous papers and holds a number of patents.

Dr. Niclas received the outstanding publications award in 1962 of the German Society of Radio Engineers.

Design of Waveguide Circulators with Chebyshev Characteristics Using Partial-Height Ferrite Resonators

JOSEPH HELSZAJN, MEMBER, IEEE

Abstract—**This paper outlines a step-by-step approach to the design of waveguide circulators using partial-height resonators, which incorporates every linear dimension of the device. The approach used consists of defining the physical variables of the ferrite region in terms of the frequency, VSWR, and bandwidth specification. It also incorporates the definition of the length and admittance level of the radial transformer. The model employed is essentially a two-mode one, with the third mode separately adjusted to exhibit an ideal electric-wall boundary condition at the terminals of the junction.**

Manuscript received August 10, 1983; revised March 5, 1984.
The author is with the Department of Electrical and Electronic Engineering, Heriot-Watt University, Edinburgh EH1 2HT, Scotland.

I. Introduction

ALTHOUGH THE 1-PORT complex gyrator circuit (operating frequency, susceptance slope parameter, loaded Q-factor, gyrator conductance) of waveguide circulators using weakly magnetized quarter-wave-long open ferrite resonators is fairly well understood [1]–[27], there is still no step-by-step procedure for their design in terms of a return loss and bandwidth specification. This is in part due to the fact that the radial impedance transformer used in these devices is a nonuniform line whose dimensions are dependent upon both the gyrator conductance and its terminal plane, and it is in part due to the difficulty in

0018-9480/84/0800-0908$01.00 ©1984 IEEE